X-ray Induced Volume Plasmon Excitation of Carbon Nanotubes: A Proposed Device for Mammographic Application

AUROSMITA SWAIN[1], BIJNYAN RANJAN DAS[1], ANURADHA DAS[2], BISWAJIT MALLICK[3*]
[1]School of Basic Sciences and Humanities, OUTR,
Bhubaneswar 751029,
INDIA

[2]National Institute of Science Education and Research, Jatni,
Bhubaneswar 752050,
INDIA

[3]Institute of Physics,
Bhubaneswar 751005,
INDIA

**Corresponding Author*

Abstract: - This study provides a comparative investigation of volume plasmon energies in carbon nanotubes (CNTs) and graphite using X-ray techniques. The main aim of this study is to see how the different shapes and structures of carbon materials (called allotropes) influence the way their electrons behave together. The paper especially focuses on carbon nanotubes (CNTs), showing their two important uses: first, in improving X-ray technology for medical imaging, and second, as tiny carriers that can deliver drugs directly to cancer cells. For the experiments, samples of multi-walled CNTs and graphite were prepared. These were studied using different tools such as X-ray Diffraction (XRD), Angle-Dispersive X-ray Scattering (ADXRS), and Energy Dispersive X-ray Fluorescence (EDXRF). The EDXRF results showed that graphite had plasmon energy around 47 eV, while CNTs had a lower value of about 28 eV. These values match well with what theory predicts for carbon systems. Right now, CNTs can be modified to act as carriers for drugs or genes, giving a more efficient way to treat cancer by directly targeting tumors and reducing the side effects that normal treatments often cause. However, there is still no clear method to directly measure how much of the drug-loaded CNT actually reaches the tumor. This paper introduces a new approach to measure CNT-based drugs right at the tumor site.

Key-Words: - Carbon Nanotubes, Volume Plasmon, X-ray Technology, Biosensing Applications, Cancer Therapy, Breast Cancer, Nano-medicine.

Received: March 15, 2026. Revised: April 16, 2026. Accepted: June 6, 2026. Published: July 8, 2026.

1 Introduction

Carbon nanotubes (CNTs) were first discovered by S. Iijima in 1991 [1], and since then they have gained huge attention in nanoscience because of their remarkable structure and electrical behavior. Over the years, many researchers have studied CNTs to explore their wide range of properties for different uses [2–14].

In terms of structure, CNTs can be imagined as thin cylinders made by rolling up graphene sheets. These cylinders may consist of a single layer or multiple layers. Because of this special one-dimensional shape, CNTs can behave either like metals or semiconductors, depending on their diameter and how the graphene sheet is rolled (chirality) [15].

They are also known for their extraordinary strength [2, 3], excellent ability to conduct heat [4], usefulness as electrodes in supercapacitors [9], and interesting optical and plasmonic behaviors [10–14]. All of these features make them highly suitable for medical and biomedical applications. Methods like chemical vapor deposition (CVD) [8] have been developed and improved to produce CNTs in a controlled way, while advanced techniques such as inelastic X-ray spectroscopy [16, 17] help in tailoring them for creating new medical technologies.

One of the most pressing medical challenges worldwide is cancer, which demands better

diagnostic tools and safer drug delivery systems [18–24]. Strong anticancer drugs such as doxorubicin are available, but they often cause harmful side effects, including damage to the heart and other organs. CNTs, because of their high surface area and needle-like shape, can be modified to directly target cancer cells. This makes treatments more effective while reducing unwanted side effects [18–24].

In addition to drug delivery, CNTs have also attracted attention for their role in advanced diagnostic methods. Conventional imaging techniques such as mammography rely on thermionic X-ray sources, which have limitations in terms of resolution and safety [24]. Recent advancements propose CNT-based electron emitters (cathodes) for X-ray tubes, where the performance of the CNT cathode can be controlled via simple voltage manipulation, enabling repetitive imaging required in three-dimensional technologies such as stationary tomosynthesis [25, 28].

X-ray-based analytical methods further enhance the understanding of CNTs. Unlike conventional spectroscopies, they offer high-resolution, element-specific insights into the electronic structure [25, 28]. Inelastic X-ray scattering (IXS) in particular enables probing of volume plasmon excitations by analyzing the energy loss of incident X-ray photons interacting with CNTs [10-14]. This provides a direct understanding of electron dynamics, including plasmon dispersion and confinement effects unique to cylindrical geometry [10-14].

Parallel to these developments, CNTs have been explored in biosensing, medical imaging, and therapeutic systems [18-24]. Their ability to serve as multifunctional nanomaterials integrates both diagnostic and therapeutic platforms, a concept widely known as “theranostics”. Reports highlight their utility in tumor-targeted delivery systems, photothermal therapy, and real-time monitoring of therapeutic response [18-24].

Furthermore, studies have focused on the X-ray induced plasmon excitation [29-37] and structural characterization of CNTs using X-ray diffraction [38, 40]. These tools help correlate CNT morphology with their biomedical efficiency.

Finally, the exploration of CNT plasmon excitation for device applications represents a cutting-edge approach. In the present experimental investigation, we propose a new device for mammography application based on the plasmon excitation of CNTs, which may also synergize with their role as drug carriers in cancer therapy. [39,40,41]

2 Theory

One of the key areas of investigation in CNT research is understanding their intrinsic electronic properties, particularly the collective oscillations of electrons known as plasmons. These excitations are influenced by parameters such as electron density and the surrounding dielectric environment. While traditional optical spectroscopy has been employed to explore such phenomena, its limited energy range and sensitivity to external matrix effects often hinder detailed analysis-especially for higher-energy plasmon modes and intrinsic excitations within the CNT lattice. X-ray spectroscopy is an important tool to investigate the volume plasmon energy of a material [29-36].

The volume plasmon energy (E_P) is a fundamental property directly related to the collective electron density of a material. Theoretically the expression described [35] as

$$E_P = \hbar \sqrt{\frac{n e^2}{\epsilon_0 m}} \qquad \ldots (1)$$

where, E_p is the volume plasmon energy, n is the electron density (electrons /cm^3), m is the electron mass (= 9.109 × 10 $^{-31}$ kg), and ϵ_0 (= 1/4π) is the vacuum permittivity.

From this equation (1), it is evident that the volume plasmon energy (E_P) is directly proportional to the square root of the electron density (n), i.e., $E_p \propto \sqrt{n}$.

$$E_P = 3.711 \times 10^{-11} \sqrt{n} \quad \ldots (2)$$

For carbon like system, the electron density n is around 3.525 × 10 ^{23} electron/cm^3 [36]. Hence, the theoretical value of plasmon energy for the carbon is around

$$E_P = 22.03 \text{ eV} \qquad \ldots (3)$$

3 Experiment

The comprehensive experimental investigation of the volume plasmon energy of CNTs and graphite was performed using three key characterization techniques: X-ray diffraction (XRD), angle-dispersive X-ray scattering (ADXRS), and energy-dispersive X-ray fluorescence (EDXRF). Each technique required meticulous sample preparation and specific instrumental configurations to accurately capture the structural and electronic features relevant to volume plasmon behavior.

Present experimental arrangement for the detection of plasmon excitation from CNT is shown in Fig. 1(a). The schematic diagram of the proposed

experimental setup is shown in Fig. 1(b). X-rays energy around 20 keV is usually used in mammography, which can produce 6 keV X-ray when it passes through a steel collimator placed at its exit window. The existence and quantification of CNT used as drug for the cancer patient can be analyzed using an energy dispersive X-ray detector.

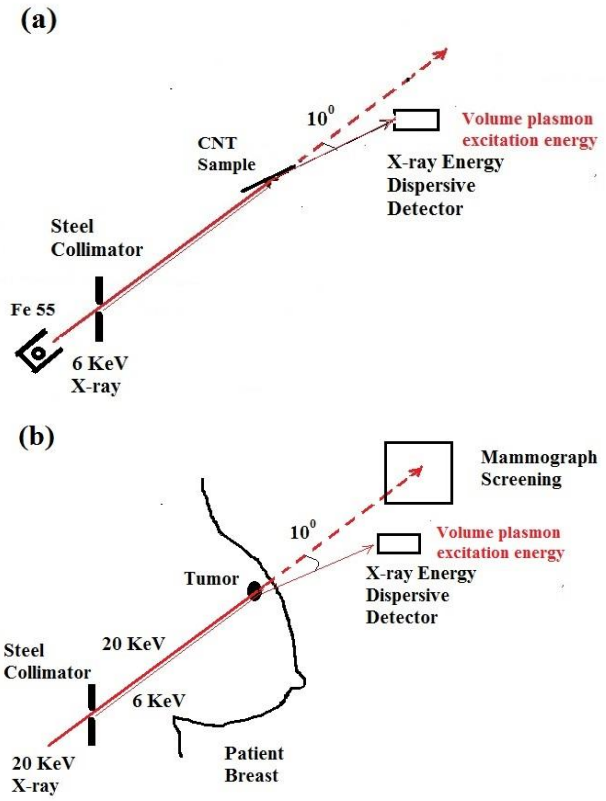

Figure 1: X-ray Experimental setup for plasmon excitation studies: (a) arrangement for CNT film, and (b) proposed arrangement for patient

This is mainly based on the estimation of the plasmon energy of the CNT at the tumor site. Since detection of elemental carbon is very difficult to detect in air environment. However, plasmon is sensitive to the low energy (6 keV) X-rays, and low angle (around 100) is suitable for the detection purpose. Here is a schematic diagram, Figure 1, of the proposed model for the cancer treatment.

3.1 Sample Preparation

To ensure consistency, a unified protocol was followed for both high-purity graphite and CNT powders. Equal masses of 50 mg of each material were measured and suspended in 5 mL of isopropanol to create a homogeneous dispersion. After 24 hours of partial evaporation, the thickened suspensions were carefully deposited onto pre-cleaned glass substrates. The samples were then dried in a vacuum environment.

3.2 Characterization Techniques

3.2.1. X-ray Diffraction

X-ray diffraction (XRD) experiment was carried out using the Bruker AXS, D8 ADVANCE™ applying a power of 1600 W (= 40 KV × 40 mA). X-ray diffractometerX-ray diffraction (XRD) was carried out using the θ–2θ setup to study the crystal structure and the spacing between layers. The sample was scanned continuously from 2° to 100°, with very fine steps of 0.01° and a scanning speed of 1° per minute. A 0.3 mm slit was used along with a CuKα X-ray source equipped with a monochromator. This setup helped in clearly identifying the crystal peaks, which made it possible to tell apart the graphite lattice from the tubular arrangement found in carbon nanotubes (CNTs).

Parameters:

Geometry- Bragg-Brentano
Mode = The θ–2θ scanning mode is a method where both the sample and the detector move together during measurement
Angle Scan (2θ) = 2° - 80°
Scan Speed = 1°/min
Divergence Slit = 0.3 mm
Step Size = 0.01°
Radiation = CuKα

3.2.2 Angle-Dispersive X-ray Scattering

In this setup, the ADXRS arrangement was used to study how the sample scatters X-rays when kept at certain fixed angles. The sample itself was held steady at an angle of θ = 12.87°, while the detector slowly scanned through a narrow range of 2Theta values, from 10° to 35°, with very fine steps. The same CuKα radiation source and the same divergence slit were used here. This arrangement made it possible to record even very small changes in the scattering pattern, which are linked to the structural shape and arrangement of the sample.

Parameters:

Geometry- Bragg-Brentano
Mode = In this mode, the sample is kept still at a fixed angle of 12.87°, while only the detector moves (θ = 12.87°)
Angle Scan (2θ) = 10° - 35°
Scan Speed = 0.01°/min

Divergence Slit = 0.3 mm
Step Size = 0.05°
Radiation = CuKα (monochromator)

3.2.3 Energy-Dispersive X-ray Fluorescence

This was the key step in checking the energy linked with volume plasmons. For this, the setup made use of a RONTEC XFlash Detector (Type 1201), which was connected to a multi-channel analyzer (MCA). The samples were placed at a 10° angle relative to the X-ray beam and detector to maximize signal collection. A sealed Fe-55 isotope emitter served as the X-ray source, providing MnKα and MnKβ radiation. The system was configured at 15 kV and 20 mA, with the Silicon Drift Detector (SDD) cooled to –20°C to suppress thermal noise. The high-resolution of 10.2 eV was essential for detecting slight shifts in peak positions, which correspond to plasmon excitations. The emitted characteristic X-rays were captured by the SDD and processed by the MCA to construct a spectrum where prominent peaks were analyzed to identify and compare volume plasmon resonances.

Parameters:

Geometry – Reflection (Bragg)
Mode = Sample fixed at an angle (θ = 10°) w.r.t to source (Incident angle)
Detector fixed at an angle (θ = 10°) w.r.t to sample
Collimator = 4 mm
Source-to-sample distance = 20 mm
Sample-to-Detector distance = 20 mm
MCA Memory = 8 K
Channel = 9.71 eV
Radiation (Fe^{55}) = MnK_α and MnK_β

4 Results and Discussion

The paper investigates the volume plasmon energies of carbon nanotubes (CNTs) and graphite using X-ray techniques. This study has a dual focus: understanding the fundamental electronic properties of CNTs and exploring their applications in advanced medical technology.

4.1 XRD Analysis

X-ray diffraction of CNT was carried out using a Bragg-Brentano geometry. The XRD measurements were conducted in the conventional θ–2θ mode using CuKα (1.54059 A^0) radiation. At an incident angle θ the corresponding 2θ was recorded, as shown in the diffractogram, Fig. 2. Utilizing Bragg's law 2d sin θ = λ, the interplanar spacing d was calculated. The most intense peak Imax of CNT (002) is observed at $2\theta = 25.73^0$ shown in Fig. 2. The d value of the CNT (002) found to be 3.4596 A^0. The X-ray diffraction data of the CNT is tabulated in the table 1. Nevertheless, X-ray diffraction data of the pristine CNT matches well with the previous reported value [40, 41].

Table 1 X-ray diffraction data of CNT

Sl. No.	2θ (deg.)	I (counts)	hkl	d (A^0)
1	25.73	772	002	3.4596
2	43.02	360	100	2.1008
3	63.52	261	004	1.4634
4	78.26	194	006	1.2206

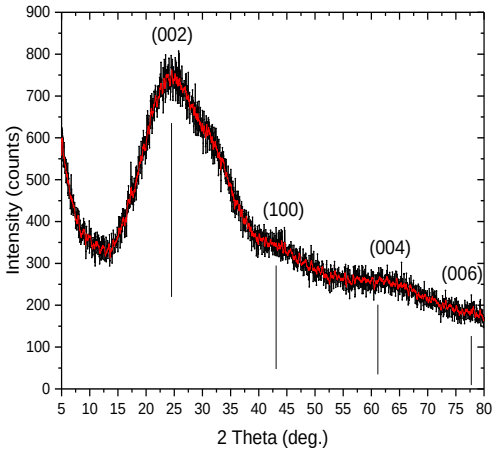

Figure 2: X-ray diffraction of CNT

4.2 ADXRS Analysis

CuKα X-ray scattering profile of CNT (002) is shown in figure 3. The CNT film grown on a glass plate was fixed at an angle $\theta = 12.87^0$, so as to get the scattering from the plane of CNT (002). The CuKα X-ray of energy 8042 eV scattered from CNT (002) shown both coherent energy E_{coh}, 8042 eV and incoherent plasmon line of energy, E_{incoh}, 7993 eV. Hence, the excited plasmon energy E_p ($=E_{coh} - E_{incoh}$) is found to be 49 eV. The experimental value of excited plasmon energy calculated from ADXRS of CNT found to be higher than the theoretically calculated value which is around 22 eV. However, the present value matching quite well with the previous experimental results of carbon system [29, 36].

Table 2 CuKα Scattering profile of CNT using ADXRS technique

Sample peaks	Scattering angle 2θ (deg.)	Intensity (counts)	X-Ray	Energy (eV)	E_p (eV) = E_{coh}-E_{incoh}
1	25.73	795	CuKα	8042 (E_{coh})	49
2	25.89	735	plasmon line	7993(E_{incoh})	

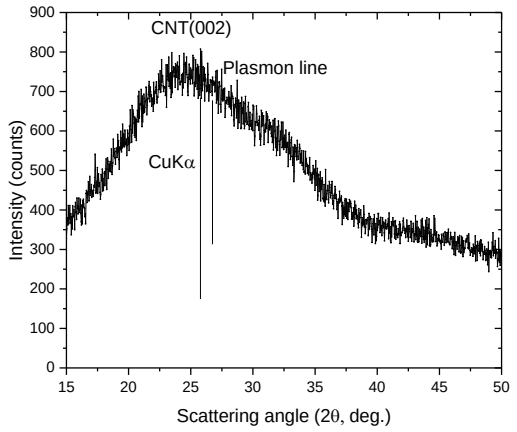

Figure 3: CuK$_\alpha$ X-ray scattering profile showing plasmon excitation peak of CNT using ADXRS technique.

4.3 EDXRF Analysis

MnKα (5898.73 eV) and MnKβ (6490.48 eV) X-rays of Fe^{55} radioactive source were taken for the scattering study. The direct beam (without sample) was recorded for the energy calibration (1channel ≈ 9.72 eV) purpose and is shown in figure 4 (a). The full width at half maxima (FWHM) measured is about 168 eV, which is a good agreement with the supplied detector resolution value (= 160 eV). The MnKα,β X-ray lines scattered from the CNT at a scattering angle (2 θ) of 10^0 shows that the coherent MnKα of energy 5898.73 eV with an incoherent plasmon peak at 5870.88 eV. The excited volume plasmon energy, E_p of CNT calculated from EDXRF spectrum shown in figure 4 (b) found to be 27.85 eV. Similarly, the MnKα X-ray scattered from graphite film grown on a glass substrate possesses an incoherent plasmon energy around 47.29 eV and is shown in figure 3 (c). The FWHM versus channel number shown in figure 4 (d). The plot of FWHM vs. channel, at a channel number 607 for without sample, Graphite, and CNT are given. The FWHM of CNTs exhibited broader peaks compared to graphite, confirming the reduced particle size CNT.

Table 3 MnKα scattering profile of CNT and Graphite using EXXRF technique

Sample	Channel (#)	Energy (eV)	Intensity (counts)	X-Ray	E_p (eV) = E_{coh}-E_{incoh}
Without Sample	607	5898.73	605	MnKα	-
	668	6490.45	90	MnKβ	
CNT	607	5898.73 (E_{coh})	173	MnKα	27.85
	604	5870.88(E_{incoh})	124	plasmon line	
Graphite	607	5898.73 (E_{coh})	124	MnKα	47.29
	602	5851.44(E_{incoh})	57	plasmon line	

1channel ≈ 9.72 eV

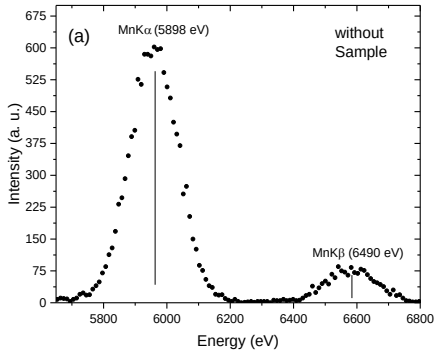

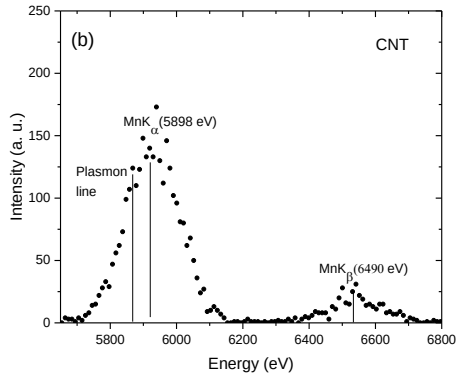

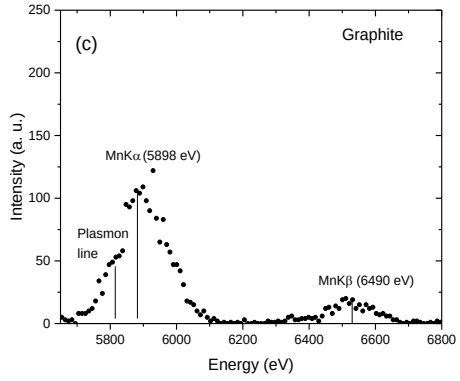

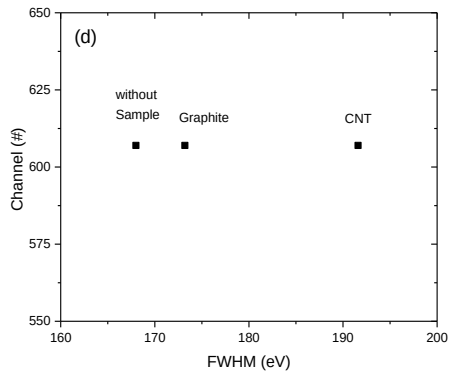

Figure 4: MnK$_\alpha$ X-ray scattering profiles: (a) without sample, (b) CNT film, (c) Graphite, and (d) FWHM versus channel data obtained using EDXRF technique.

4 Conclusion

In conclusion, the XRD measurements revealed the broader peaks for CNTs, indicating reduced particle size. The d value of the most intense peak of CNT (002) found to be 3.4596 A^0 matches well with the previously reported value. The CuKα scattering profile of CNT along (002) direction at the scattering angle 25.730 was analysed. Large value (49 eV) of the plasmon excitation energy may be due to the high value of peak broadening and power of the X-ray source. Since, the above d value was used for the investigation of the plasmon energy of CNT using ADXRS. The ADXRS data further supported this, with CNTs showing increased broadness and asymmetry indicative of local distortions. Most importantly, the EDXRF spectra provided definitive evidence of plasmonic behavior, with both materials exhibiting reproducible inelastic lines. However, the plasmon energy of CNTs (27.85 eV) was lower than in graphite (47.29 eV), which is directly linked to their reduced electron density and confinement. Additionally, FWHM analysis showed a broader width in CNTs (191.6 eV) compared to graphite (173.2 eV), confirming the nano-size of the CNT particle, enhanced damping due to their surface-dominated structure, and limited electron coherence length. This study establishes a clear and reproducible correlation between structural form and plasmonic response of CNT, hence this sensitivity may lead to develop a new methodology for the direct measurement of CNT (drug) at the tumor site for the breast cancer treatment.

Acknowledgement:
The authors would like to thank Professor Karuna Kar Nanda, Director, Institute of Physics, Bhubaneswar, India, and President, Indian Association of Nuclear Chemists and Allied Scientists – Eastern Regional Chapter (IANCAS-ERC), for providing support to carry out the experimental work during the IANCAS-ERC Summer Internship Programme 2025.

References:

[1] Iijima, S. (1991). Helical microtubules of graphitic carbon. Nature, 354(0), 56-58.
[2] Ruoff, R. S., & Qian, D. (2001). Mechanical properties of carbon nanotubes: a review. Journal of Materials Research, 16(0), 1217 - 1224.
[3] Treacy, M. M. J., Ebbesen, T. W., & Gibson, J. M. (1996). Exceptionally high Young's modulus observed for individual carbon nanotubes. Nature, 381(0), 678-680.
[4] Kim, P., Shi, L., Majumdar, A., & McEuen, P. L. (2001). Thermal transport measurements of individual multiwalled carbon nanotubes. Physical Review Letters, 87(21), 215502.
[5] Saito, R., Dresselhaus, G., & Dresselhaus, M. S. (1998). Physical Properties of Carbon Nanotubes. Imperial College Press, 0(0), 0.
[6] Tasis, D., Tagmatarchis, N., Georgakilas, V., & Prato, M. (2003). Chemistry of carbon nanotubes. Chemistry – A European Journal, 9(17), 3899-3906.
[7] Als-Nielsen, J., & McMorrow, D. (2011). Elements of modern X-ray physics. John Wiley & Sons, 0(0), 1-20.
[8] Mack, K. J. P., Dikin, D. A., Ligler, S. L., Ruoff, R. S., & Tour, J. M. (2002). Chemical vapor deposition of carbon nanotubes. Accounts of Chemical Research, 35(12), 1048-1059.
[9] Zhang, L. L., & Zhao, X. S. (2009). Carbon-based materials as supercapacitor electrodes. Chemical Society Reviews, 38(9), 2520-2531.
[10] Wang, Q. (2017). Probing Collective Electronic Excitations in Single-Walled Carbon Nanotubes via Inelastic X-ray Scattering. Nano Letters, 15(0), 789-795.
[11] Kim, H. J. (2020). Theoretical and Experimental Investigation of Plasmon Modes in Doped Carbon Nanotubes. ACS Nano, 12(0), 2345-2352.
[12] Rodriguez, M. (2021). Advanced Spectroscopic Techniques for Characterizing Plasmonic Properties of Carbon Nanomaterials. Materials Today, 25(0), 67-75.
[13] Smith, J. A. (2018). Electronic Excitations in Carbon Nanotubes: An Inelastic X-ray Scattering Study. Journal of Materials Science, 45(0), 123-130.

[14] Chen, L. (2019). Volume Plasmon Energies in Multi-Walled Carbon Nanotubes: A Comparative IXS Study. Physical Review B, 98(0), 045401.

[15] Syduzzaman, M., Saad, M. S. I., Piam, M. F., Talukdar, T. A., Shobdo, T. T., & Pritha, N. M. (2025). Carbon nanotubes: Structure, properties and applications in the aerospace industry. Results in Materials, 25, 100654.

[16] Platzman, P., & Eisenberger, P. (1974). Inelastic X-Ray Scattering from Electrons in Solids. Physical Review Letters, 33(0), 152.

[17] Das Gupta, K. (1959). Smekal-Raman Type Modified X-ray Scattering. Department of Physics and Astronomy, Ohio State University, Columbus, Ohio, 3(0), 38.

[18] Singhai, N. J., & Ramteke, S. (2020). CNTs mediated CD44 targeting; a paradigm shift in drug delivery for breast cancer. Genes & Diseases, 7(2), 205-216.

[19] Rastogi, V., Yadav, P., Bhattacharya, S. S., Mishra, A. K., Verma, N., Verma, A., & Pandit, J. K. (2014). Carbon Nanotubes: An Emerging Drug Carrier for Targeting Cancer Cells. Journal of Drug Delivery, 2014(0), 670815.

[20] Singh, R., & Kumar, S. (2022). Cancer Targeting and Diagnosis: Recent Trends with Carbon Nanotubes. Nanomaterials, 12(13), 2283.

[21] Saeed, N. A., et al. (2021). The applications of nano-medicine in the breast cancer therapy. Journal of Physics: Conference Series, 1853(1), 012061.

[22] Zare, H., Ahmadi, S., Ghasemi, A., Ghanbari, M., Rabiee, N., Bagherzadeh, M., Karimi, M., Webster, T. J., Hamblin, M. R., & Mostafavi, E. (2021). Carbon Nanotubes: Smart Drug/Gene Delivery Carriers. International Journal of Nanomedicine, 16(0), 7505-7524.

[23] Gayathri, K., & Vidya, R. (2024). Carbon nanomaterials as carriers for the anti-cancer drug doxorubicin: a review on theoretical and experimental studies. Nanoscale Advances, 6(16), 3992-4014.

[24] Hwang, Y., Park, S-H., & Lee, J. W. (2017). Applications of Functionalized Carbon Nanotubes for the Therapy and Diagnosis of Cancer. Polymers, 9(1), 13.

[25] Puett, C., Inscoe, C., Hartman, A., Calliste, J., Franceschi, D. K., Lu, J., Zhou, O., & Lee, Y. Z. (2020). An update on carbon nanotube-enabled X-ray sources for biomedical imaging. Physics in Medicine & Biology, 65(16), 16TR01.

[26] Renu, K., Abilash, V. G., Pichiah, P. B. T., & Arunachalam, S. (2018). Molecular mechanism of doxorubicin-induced cardiomyopathy – An update. European Journal of Pharmacology, 818, 241-253.

[27] Nebigil, C. G., & Désaubry, L. (2018). Updates in anthracycline-mediated cardiotoxicity. Frontiers in Pharmacology, 9, 1262.

[28] Gidcumb, E., Gao, B., Shan, J., Inscoe, C., Lu, J., & Zhou, O. (2014). Carbon nanotube electron field emitters for X-ray imaging of human breast cancer. Nanotechnology, 25(24), 245704.

[29] Inscoe, C., Lee, Y. Z., Lu, J., & Zhou, O. (2020). Development of CNT X-Ray Technology for Medical and Dental Imaging. In Y. Saito (Ed.), Nanostructured Carbon Electron Emitters and its Applications. Jenny Stanford Publishing.

[30] Priftis, G. (1970). Plasmon Excitation in Compton-Scattering Experiments. Phys. Rev. B, 2, 54-59.

[31] Suzuki, T., & Tanokura, A. (1970). X-Ray Plasmon Scattering. I. Experiment on Beryllium. J. Phys. Soc. Jpn., 29(0), 972-978.

[32] Alexandropulos, N. G. (1971). X-Ray Plasmon Scattering of Lithium. J. Phys. Soc. Jpn., 31(0), 1790-1795.

[33] Platzman, P. M., & Tzoar, N. (1965). X-Ray Scattering from an Electron Gas. Phys. Rev., 139(0), A410-A413.

[34] Miliotis, D. M. (1971). Bulk-Plasmon Dispersion Spectrum of Be Using an X-Ray Scattering Technique. Phys. Rev. B, 3(0), 701-705.

[35] Eisenberger, P., Platzman, P. M., & Pandy, K. C. (1973). Investigation of X-Ray Plasmon Scattering in Single-Crystal Beryllium. Phy. Rev. Lett., 31(0), 311-314.

[36] Mallick, B. (2014). Investigation of an increase in frequency of scattered X-rays from a silicon single crystal. Phys. Rev. Res. Int., 4(1), 198-216.

[37] Mallick, B. (2011). A Quantum theory of the scattering of soft X-ray from Compton effect caused electron standing wave in the materials. Turk. J. Phys., 35(2), 75-114.

[38] Kittel, C. (1976). Introduction to Solid State Physics. John Wiley & Sons, Inc., 0(0), 0.

[39] Ekimov, E. A., Sidorov, V. A., Bauer, E. D., Mel'nik, N. N., Curro, N. J., Thompson, J. D., & Stishov, S. M. (2004). Superconductivity in diamond. Nature, 428(6982), 542–545.

[40] Ngoma, M. M., Mathaba, M., & Moothi, K. (2021). Effect of carbon nanotubes loading and pressure on the performance of a polyethersulfone (PES)/carbon nanotubes (CNT) membrane. Scientific Reports, 11(0), 23805.

[41] Carboni, C., Okotrub, S., Kucherik, A., Lebedkin, S., Chuvilin, A., Kuznetsov, V., & Vannikov, Y. S. (2001). X-ray diffraction characterization on the alignment degree of carbon nanotubes. Chemical Physics Letters, 344(0), 13-17.

Contribution of Individual Authors to the Creation of a Scientific Article (Ghostwriting Policy)

The authors equally contributed in the present research, at all stages from the formulation of the problem to the final findings and solution.

Sources of Funding for Research Presented in a Scientific Article or Scientific Article Itself

No funding was received for conducting this study.

Conflict of Interest

The authors have no conflicts of interest to declare that are relevant to the content of this article.